DOI: 10.1016/j.compscitech.2014.02.015

Hybrid Carbon Fibre – Carbon Nanotube Composite Interfaces

S.-Y. Jin[1], R.J. Young[1], S.J. Eichhorn[*2]

1. Materials Science Centre, School of Materials, University of Manchester, Grosvenor Street, Manchester, M13 9PL, UK.

2. College of Engineering, Maths & Physical Sciences, Physics Building, University of Exeter, Stocker Road, Exeter, Devon, EX4 4QL, UK.

Abstract

Both low and high modulus carbon fibres are coated with carboxylated single wall carbon nanotubes (SWNTs). It is shown that it is then possible to follow, for the first time, the local deformation of low modulus carbon fibres and composite interfaces using Raman spectroscopy. By deforming coated single carbon fibre filaments in tension, and following the shift in the position of a band located at ~2660 cm^{-1} (2D band) it is possible to calibrate the local stress state of a fibre embedded in an epoxy resin. To follow the interface between the fibres and the epoxy resin, a thin film model composite is used. Point-to-point variation of stress along a single fibre, both inside and outside the resin, is recorded and stress transfer models are used to determine the interfacial shear stress (ISS). Values of the ISS (~20 MPa) are obtained for the thin film model composites for untreated high modulus fibres. A beneficial interfacial effect of the presence of SWNTs on the surface of the high modulus carbon fibre samples is demonstrated resulting in an increase in the maximum ISS (>30 MPa) compared to uncoated samples. Similarly coated low modulus fibres exhibit a very high ISS (>50 MPa). These increases are attributed to an enhanced contact between the resin and the

[*] Corresponding Author. Tel. : +44 0 1392 72 5515; fax: +44 0 1392 264 111. *E-mail address:* s.j.eichhorn@exeter.ac.uk (S.J. Eichhorn)

fibres due to an increased surface area as a result of the nanotubes and additional bonding caused due to the presence of carboxylate groups.

Keywords: A: Carbon nanotubes; A: Hybrid composites; C: Stress Transfer; D: Raman Spectroscopy

1. Introduction

There has been an increase in interest in carbon fibres in recent times due to their widening use in the aerospace, automotive, sports equipment and wind/tidal energy sectors. A range of carbon fibres are currently commercially available with mechanical properties ranging from low to high modulus and strength. Critical to their performance in a composite material is the interface between the fibre and the resin.

A number of groups have attempted to graft carbon nanotubes to the surface of carbon fibres [1-4] with the aim of improving the interface with a resin material. Of particular note, the interface between carbon fibres and a polymer matrix material has been recently reported to be enhanced by using carbon nanotubes (CNT) [5]. Interfacial shear stresses were recorded using single fibre fragmentation in a PMMA matrix and found to increase from 12.5 MPa for an as received fibre to 15.8 MPa for a CNT grafted fibre. The formation of hierarchical composites using carbon nanotubes to enhance composite interfaces has recently been reviewed [6].

Raman spectroscopy has been widely used to follow the deformation micromechanics of both carbon fibres [7-9] and composites [10, 11]. In order to do this the position of the 2D band, located at ~2660 cm^{-1}, is followed as a function of tensile (or compressive) deformation on a single carbon fibre filament. The slope of a linear regression to these

data is then used as a calibration of the local stress state in a model composite, allowing point-to-point mapping to take place [10, 11]. In lower modulus carbon fibres the 2D band is typically absent, and so stress mapping and interfacial analysis is more difficult. Carbon nanotubes have been coated onto fibres from which Raman spectroscopic analysis of local stress states is not possible e.g. glass [12-14]. Here the nanotubes can be directly deposited onto the fibre, or incorporated into a silane coating.

In the present work we use the approach of coating the surface of both high and low modulus carbon fibres with SWNTs. It is shown for the first time that point-to-point stress mapping of a low modulus carbon fibre can be obtained from within a model composite geometry. The positive effect of the presence of SWNTs at the interface is demonstrated, giving a means for improving the properties of composites reinforced with low modulus carbon fibres.

2. Experimental Methods

2.1 Materials

Two commercial grades of carbon fibre were used for this study; namely a high modulus carbon fibre (M46J) provided by Toray and a low modulus fibre (Tenax-J) by Toho-Tenax. Each fibre was used as-received and had no pre-treatment of its surface. Carboxylic acid treated single walled carbon nanotubes (SWNTs) were provided by Sigma Aldrich (Sigma Aldrich, Dorset, UK). The technical data sheet for these SWNTs states that they have diameters in the range 1.3 – 1.5 nm, lengths in the range 500-1500 nm and that they contain < 15 wt.% metals. The epoxy resin used as a matrix material for the model composites was provided by Vantico, Polymer Specialties, UK. The

formulation is a two part curing system of a resin (LY5052) containing 34–42% butanediol diglycidyl ether and 60–70% epoxy phenol-novolac resin and a hardener (HY5052) comprised 35% isophorone diamine, 50–60% 2,2-dimethyl-4,4-methylenebis (or cyclohexylamine) and 1–5% 2,4,6-tris (or dimethylaminomethyl) phenol. The silane coupling agent used in this study was 3-aminopropyl-triethoxysilane which is supplied by Avocado Research Chemicals, UK. A release agent named Ambersil Formula 10 was used, which is a dry film, non-silicone mould release agent and was provided by Ambersil House, UK.

2.2 Model Composite Preparation

Single carbon fibre filaments were removed from a bundle using tweezers and placed over the window of a cardboard testing frame. Each end of the fibre was glued to the cardboard using an Araldite^{TM} epoxy resin and allowed to cure. To coat the single fibres with SWNTs a 0.1% by weight dispersion of nanotubes in ethanol was sonicated for 2 hours. A 1.5 vol.% silane solution was also prepared, stirred and hydrolysed. These two solutions were mixed in a 1:1 ratio and stirred magnetically for 30 minutes. After that the fibre card samples were soaked in this mixture for 20 minutes, and then removed and heated at a temperature of 120°C for 2 hours. These samples then just had one single silane layer containing SWNTs, without the presence of an epoxy layer. Samples were then further coated with a thin layer of epoxy resin by placing them in the epoxy/hardener mixture for 5 min, followed by hot curing.

A thin-film epoxy resin-fibre system was prepared as a model composite to determine the properties of the interface. To prepare these samples, a small glass coverslip was

placed below the fibre in the middle of a testing card window, supported by two cardboard strips to prevent them from applying load to the fibre before testing or rotating during mechanical deformation (see Figure 1). After that a small droplet of epoxy resin was applied to the surface of the glass slide and another glass slide was placed on top of the first one, sandwiching the fibre between the two. Adjustments were also made to the position of the slides so that they were in line with each other as much as possible to overcome edge effects. This approach has been previously reported by Mottershead and Eichhorn, 2007 [15]. These model composites were placed with a room with a controlled environment (temperature of 23 °C and 50% humidity) for 7 days to make sure they were fully cured.

2.3 Scanning Electron Microscopy (SEM)

Ten single carbon fibre filaments were randomly selected from a bundle to ensure accurate and representative mean diameters and surface morphologies were obtained. Each fibre filament was placed horizontally onto an adhesive carbon pad which was attached onto an aluminium SEM stub. In order to obtain images of the fibre ends, filaments were attached in a vertical position to some conductive copper tape. A bundle of fibres was sandwiched by another piece of copper tape to ensure they stood firmly and perpendicularly on the SEM stub. In order to obtain images a Phillips XL-30 FEG-SEM (Field Emission Gun Scanning Electron Microscope) was used with operating voltages of 8 - 10 kV.

2.4 Mechanical Testing of Single Fibres

An Instron™ 1120 test machine was used to perform tensile tests on single filaments. These filaments were mounted onto testing cards, as previously described, and conditioned in a controlled temperature and humidity environment (temperature of 23 °C and 50% humidity) for 24 hours prior to testing. Samples were tested at a rate of 10% of the gauge length per minute. Gauge lengths in the range 10 - 100 mm were used in order to account for defects in terms of fibre strength and end effects and machine compliance. A full-scale load of 0.2 N was used, with a 1N load cell as the transducer. This transducer was calibrated before testing and 20 samples for each fibre type were tested to obtain mean mechanical property data.

2.5 Raman spectroscopy of Single Fibres and Model Composites

In order to collect Raman spectra a Renishaw system-1000 spectrometer was used. To excite Raman scattering from single carbon fibre filaments a He-Ne laser ($\lambda = 633$ nm) was used. This laser was focussed onto the fibres using a 50× long working distance objective lens housed within a Olympus BH-2 optical microscope. The laser spot size on the sample was ~2 μm in diameter. In order to prevent heating induced by the laser, a minimum laser power of 25% (full power 0.25mW) was used in this study. The polarisation was set in a 'VV' configuration; this is where the laser is polarised parallel to the tensile axis of the fibres both in free air and in the composite and the analyser was set to collect parallel polarised scattered radiation.

Spectra were recorded from single fibres using a range of collection times. For uncoated samples an exposure time of 20 seconds with 2 accumulations was adequate to obtain clear spectra from the fibres. When coated with SWNTs the exposure time was reduced

to 10 seconds since spectra of equal resolution could be obtained due to a strong resonant Raman effect. We sought to reduce the exposure time to reduce possible heating effects. The effect of exposure time on the position of Raman bands was tested using long times at the power used. We found this effect to be minimised using these values while not compromising resolution. Each spectrum was fitted in order to find its peak position using a mixed Gaussian/Lorentzian function and an algorithm based on the work of Marquardt [16].

3. Results and Discussion

3.1. Scanning Electron Microscopy of Carbon Fibres

Typical electron micrographs of both fibre ends and free filament lengths are shown in Figure 2. It can be seen from Figs 2a and 2b that the fibres have a rough serrated surface with 'grooves' running along their lengths. Figs. 1c and 1d show that the fibres have a near circular cross section. Measurements of the fibre diameters yielded values of 5.23 ± 0.20 μm and 5.35 ± 0.30 μm for the high and low modulus fibres respectively.

Figure 3 reports images of the filaments with the SWNTs in the sizing on the fibre surface (Fig. 3a) and after an epoxy resin layer has been added (Fig. 3b). The SWNTs are clearly visible and are non-aligned on the surface of the fibre (Fig. 3a). When the filaments have been coated, and hot-cured, the resultant diameter is reduced slightly, and the SWNTs are encapsulated in the resin and no longer visible (Fig. 3b).

3.2 Mechanical Properties of Single Fibres

Typical stress-strain curves for both fibre types are reported in Figure 4. Both the high and the low modulus fibres exhibit almost linear stress-strain behaviour, with a slight

strain hardening occurring at higher strains; this is typical behaviour for carbon fibres. Mean values of the mean stress at failure, Young's modulus and strain to failure were determined from these curves; values are reported in Table 1. All values were obtained by extrapolation to infinite gauge length for modulus and zero gauge length for breaking stress and strain. Clearly from these data the high modulus fibre has almost double the Young's modulus of the low modulus fibre. The strength on the other hand of the high modulus fibre is significantly lower than that of the low modulus filaments. Strain to failure of the low modulus fibre is almost twice that of the high modulus fibre.

3.3. Raman spectroscopy of Single Fibres and Model Composites

Typical Raman spectra from the fibres and SWNTs are shown in Figure 5. The high modulus carbon fibre (Fig. 5a) has characteristic bands located at ~1340 cm^{-1} (D-band), ~1580 cm^{-1} (G-band) and ~2660 cm^{-1} (2D-band). The D-band is related to the breathing mode of the six-fold aromatic ring near the basal edge and the G-band is considered to be an in-plane bond stretching motion of sp^2-hybridised C atoms [17]. The Raman spectra from low modulus carbon fibres are characteristically noisy, with only a D and a G-band present (Fig. 5b). Previous research has shown that it is only possible to carry out stress analysis using shifts in the position of the 2D band, hence the need to coat the low modulus fibres with SWNTs. A typical spectrum of the same fibre type coated with SWNTs is shown in Figure 5c. The 2D peak is visible even with the low loading of SNWTs in the resin/sizing layer. The presence of this peak in the Raman spectrum enables mapping of local stress of a fibre embedded in a model composite.

Clear shifts in the peak position of the 2D Raman band emanating from the pristine high modulus carbon fibre (Fig. 6a) and SWNTs coated on a low modulus carbon fibre (Fig.

6b) are obtained. Similar shifts were obtained for a high modulus carbon fibre coated with SWNTs (data not shown). Detailed shift data for the high modulus carbon fibre without the presence of carbon nanotubes is shown in Figure 6c. A linear regression to these data yielded a slope of -5.8 cm^{-1} GPa^{-1}. A typical detailed shift in the position of the 2D Raman band for a low modulus fibre coated with SWNTs is shown in Fig. 6c. A linear regression to these data yielded a value of the slope of -4.8 ± 0.2 cm^{-1} GPa^{-1} which was subsequently used to determine point-to-point stress in the model composite samples.

Point-to-point stress mapping across a thin-film model composite, both along free fibre lengths and within the interfacial region with an epoxy resin have been carried out. According to a theory previously developed for this model composite system [15, 18] the local fibre stress (σ_f) should vary within the limits -L to +L along the length of the interface according to the equation

$$\sigma_f = \sigma_{app} \frac{\cosh(nx/r_f)}{\cosh(nL/r_f)} \quad (1)$$

where σ_{app} is the stress applied to the fibre, n is a fitting parameter, x is the distance along the fibre within the droplet and r_f is the fibre radius. To find the interfacial shear stress (τ) the force balance equation

$$\tau = \frac{r_f}{2} \frac{d\sigma_f}{dx} \quad (2)$$

can be used to obtain the expression (from Eqn. 1)

$$\tau = \sigma_{app} \frac{n}{2} \frac{\sinh(nx/r_f)}{\cosh(nL/r_f)} \quad (3)$$

Data obtained from a model composite incorporating a high modulus carbon fibre are shown in Figure 7. These data are fitted using Equation 1 in Figure 7a showing close agreement with the theory. The fibre stress is seen to decrease dramatically along the embedded length, falling to a minimum (near zero) value along the central region. This decrease is due to a transfer of stress from the fibre to the resin. Closer inspection of the region where the decay occurs (Fig. 7b) indicates that debonding is taking place. A debond of the fibre from the resin is typified by a linearisation of the shift data leading to a constant shear stress which is assumed in this case to be entirely frictional. At a fibre stress of 0.9 GPa the fibre appears to be almost fully bonded, with small debonded region (~0.2 mm) progressing from the edge of the fibre-matrix interface. At increasing levels of fibre stress this debond progresses to a length of ~0.8 mm at the highest stress level (2.8 GPa). To determine the shear stress along a debonded length of fibre the data are fitted using the equation

$$\sigma_f = -\frac{2\tau}{r_f} x + \sigma_0 \quad (4)$$

where σ_0 is a constant and is taken as the stress ahead of the debonded region. The slope of the fitted equation ($-2\tau/r_f$) is then used to determine the shear stress. Both equations 1

and 4 are fitted to the data in Figure 7b. Interfacial shear stress values are reported in Figure 7c. The maximum interfacial shear stress for this model composite (22.5 ± 0.2 MPa) is found at one end of a fully bonded region at a fibre stress of 1.8 GPa just prior to extensive debonding of the fibre from the matrix. This interfacial shear stress value is less than the yield stress of the resin (~40-50 MPa) and is comparable to other values reported in the literature. Values of ~26 MPa have been reported for a high modulus T50 carbon fibre undergoing fragmentation in an epoxy resin model composite [10]. Similarly a value of ~20 MPa was found for the same model composite system [19]. When SWNTs are present at the high modulus carbon fibre surface (Figure 8), the interface remains fully bonded. The point-to-point stress data are again fitted using Equation 4 (Fig. 8a). Closer inspection of the interfacial region near to the edge of the fibre-matrix interface reveals (Fig. 8b) that the data follow Equation 4, suggesting that the interface remains intact. Indeed, the maximum shear stress obtained for this system (Fig. 8c) is found to be 38.4± 0.1 MPa. This increase in shear stress (~72%) suggests that the presence of the SWNTs leads to an enhancement of the interface between the resin and the fibre. The reasons why this might take place are due to the increase in the surface area and therefore closer contact with the resin due to the presence of the SWNTs. The roughness of the fibre surface may also increase due to the presence of SWNTs, leading to higher shear stress at the interface. The SWNTs used in this study are also carboxylated. The presence of carboxylate groups at the surface of the fibres may induce additional reactions and additional covalent bonding with the resin, thus enhancing the shear stress. Possible reactions that may occur are given in Figure 9.

The interface between a low modulus carbon fibre and an epoxy resin has been mapped for the first time and the data are presented in Figure 10. Again the data seem to be best

fitted using Equation 1 (Fig. 10a). On closer inspection the interface appears to remain intact up to the very highest stress level (3 GPa), at which point a small debond occurs (~0.5 mm; Fig. 10c). A maximum interfacial shear stress value is obtained using Equation 3 of 51.1 ±0.2 MPa, which is higher than the high modulus fibre also treated with SWNTs. This value is also higher than an plasma treated high modulus carbon fibre (~40 MPa) [19]. Yang *et al.* [20] report values in excess of 80 MPa for nanotube treated carbon fibres, using pull-out and fragmentation tests. Zhang *et al.* [4] report values in excess of 100 MPa. Such high values seem inconceivable given that they vastly exceed the typical shear yield strength of an epoxy resin. It is possible though that the presence of nanotubes within the interface zone may also increase the shear yield strength of the resin, but this remains a topic for future study.

4. Conclusions

It has been shown that by coating both high and low modulus carbon fibres with SWNTs the local stress state of single filaments in a model composite can be determined using a Raman spectroscopy method. This effect is demonstrated for the first time for low modulus carbon fibres, which may find use in medium stiffness-high volume applications *e.g.* automotive, wind, sports goods. By fitting a model to the stress profiles obtained from the model composites it is possible to determine the interfacial shear stress along the interface. By coating the fibres using SWNTs it is demonstrated that an enhancement of the interface occurs leading to a significant increase in the interfacial shear stress. This approach is therefore demonstrated as a means for both interface enhancement and for monitoring local stress between a low modulus carbon fibre and epoxy resin.

References

[1] He XD, Zhang FH, Wang RG, Liu WB. Preparation of a carbon nanotube/carbon fiber multi-scale reinforcement by grafting multi-walled carbon nanotubes onto the fibers. Carbon. 2007;45(13):2559-2563.

[2] Mei L, He XD, Li YB, Wang RG, Wang C, Peng QY. Grafting carbon nanotubes onto carbon fiber by use of dendrimers. Materials Letters. 2010;64(22):2505-2508.

[3] Bekyarova E, Thostenson ET, Yu A, Kim H, Gao J, Tang J, et al. Multiscale carbon nanotube-carbon fiber reinforcement for advanced epoxy composites. Langmuir. 2007;23(7):3970-3974.

[4] Zhang FH, Wang RG, He XD, Wang C, Ren LN. Interfacial shearing strength and reinforcing mechanisms of an epoxy composite reinforced using a carbon nanotube/carbon fiber hybrid. Journal of Materials Science. 2009;44(13):3574-3577.

[5] Qian H, Bismarck A, Greenhalgh ES, Shaffer MSP. Carbon nanotube grafted carbon fibres: A study of wetting and fibre fragmentation. Composites Part a-Applied Science and Manufacturing. 2010;41(9):1107-1114.

[6] Qian H, Greenhalgh ES, Shaffer MSP, Bismarck A. Carbon nanotube-based hierarchical composites: a review. J Mater Chem. 2010;20(23):4751-4762.

[7] Huang YL, Young RJ. Structure-Property Relationships In Carbon-Fibers. Institute Of Physics Conference Series. 1993(130):319-322.

[8] Huang Y, Young RJ. Effect Of Fiber Microstructure Upon The Modulus Of Pan-And Pitch-Based Carbon-Fibers. Carbon. 1995;33(2):97-107.

[9] Tanaka F, Okabe T, Okuda H, Kinloch IA, Young RJ. The effect of nanostructure upon the compressive strength of carbon fibres. Journal of Materials Science. 2013;48(5):2104-2110.

[10] Huang YL, Young RJ. Analysis Of The Fragmentation Test For Carbon-Fiber Epoxy Model Composites By Means Of Raman-Spectroscopy. Composites Science And Technology. 1994;52(4):505-517.

[11] Huang YL, Young RJ. Interfacial micromechanics in thermoplastic and thermosetting matrix carbon fibre composites. Composites Part A-Applied Science And Manufacturing. 1996;27(10):973-980.

[12] Sureeyatanapas P, Young RJ. SWNT composite coatings as a strain sensor on glass fibres in model epoxy composites. Composites Science and Technology. 2009;69(10):1547-1552.

[13] Sureeyatanapas P, Hejda M, Eichhorn SJ, Young RJ. Comparing single-walled carbon nanotubes and samarium oxide as strain sensors for model glass-fibre/epoxy composites. Composites Science and Technology. 2010;70(1):88-93.

[14] Liu L, Ma PC, Xu M, Khan SU, Kim JK. Strain-sensitive Raman spectroscopy and electrical resistance of carbon nanotube-coated glass fibre sensors. Composites Science and Technology. 2012;72(13):1548-1555.

[15] Mottershead B, Eichhorn SJ. Deformation micromechanics of model regenerated cellulose fibre-epoxy/polyester composites. Composites Science and Technology. 2007;67(10):2150-2159.

[16] Marquardt DW. An algorithm for least-squares estimation of non-linear parameters. Journal of the Society for Industrial and Applied Mathematics. 1963;11(2):431-441.

[17] Ferrari AC, Robertson J. Interpretation of Raman spectra of disordered and amorphous carbon. Physical Review B. 2000;61(20):14095-14107.

[18] Eichhorn SJ, Bennett JA, Shyng YT, Young RJ, Davies RJ. Analysis of interfacial micromechanics in microdroplet model composites using synchrotron microfocus X-ray diffraction. Composites Science and Technology. 2006;66(13):2197-2205.

[19] Montes-Moran MA, Young RJ. Raman spectroscopy study of high-modulus carbon fibres: effect of plasma-treatment on the interfacial properties of single-fibre-epoxy composites - Part II: Characterisation of the fibre-matrix interface. Carbon. 2002;40(6):857-875.

[20] Yang L, He XD, Mei L, Tong LY, Wang RG, Li YB. Interfacial shear behavior of 3D composites reinforced with CNT-grafted carbon fibers. Composites Part a-Applied Science and Manufacturing. 2012;43(8):1410-1418.

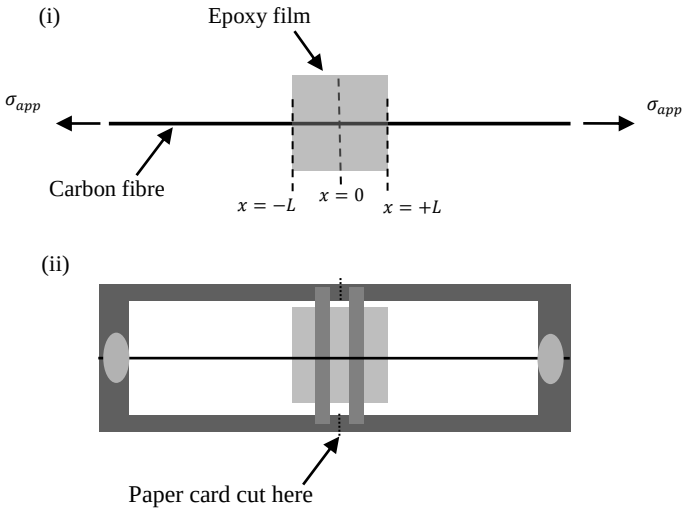

Figure 1 Schematics of (i) a single carbon fibre-epoxy film model composite indicating the applied fibre stress (σ_{app}), the length along the interface (x) from $-L$ to $+L$ and (ii) the testing card used to deform the model composite sample.

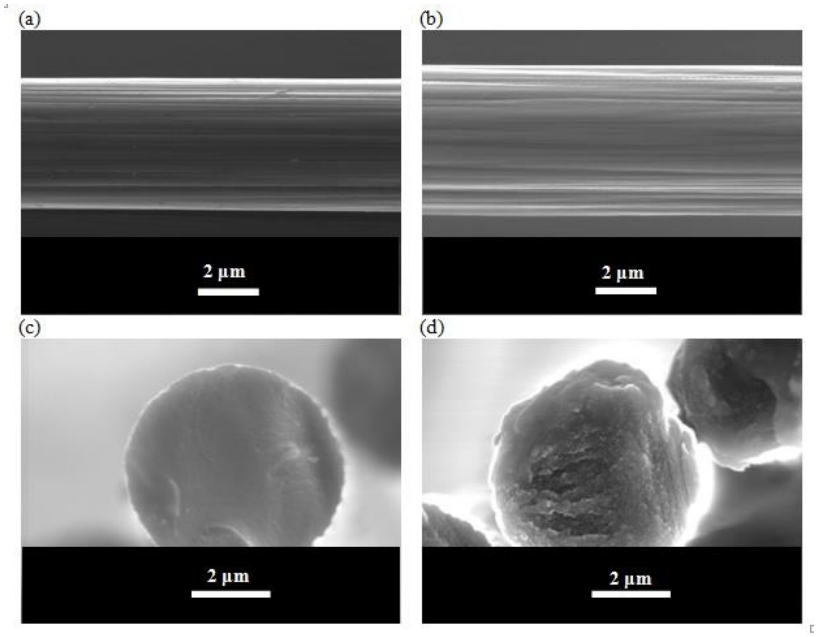

Figure 2 Typical Scanning Electron Microscope (SEM) images of carbon fibres; (a) high modulus and (b) low modulus filaments along a free fibre length; (c) high modulus and (d) low modulus cross-sections

(a)

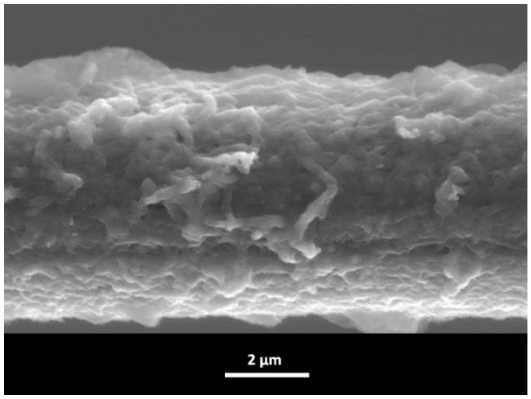

(b)

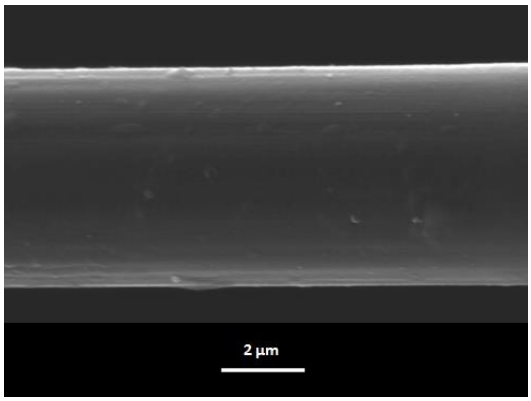

Figure 3 Typical Scanning Electron Microscope (SEM images of (a) a low modulus carbon fibre coated with single wall carbon nanotubes and (b) the same fibre further coated with an epoxy resin.

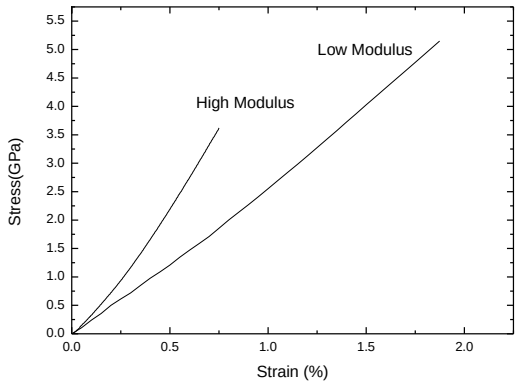

Figure 4 Typical stress-strain curves for high and low modulus carbon fibres

(a)

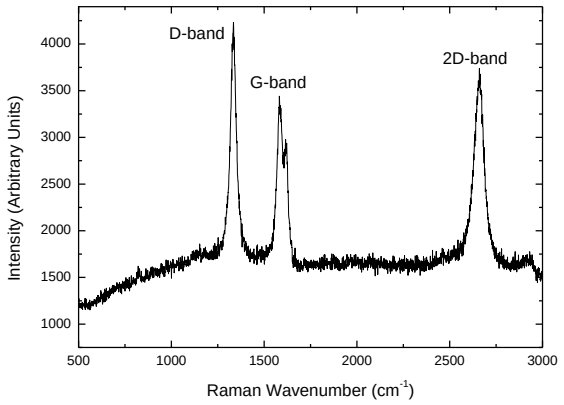

(b)

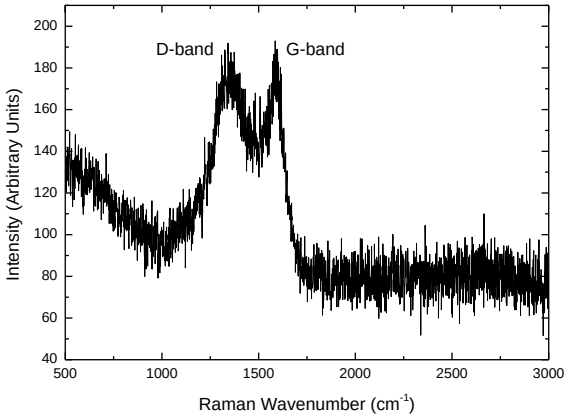

(c)

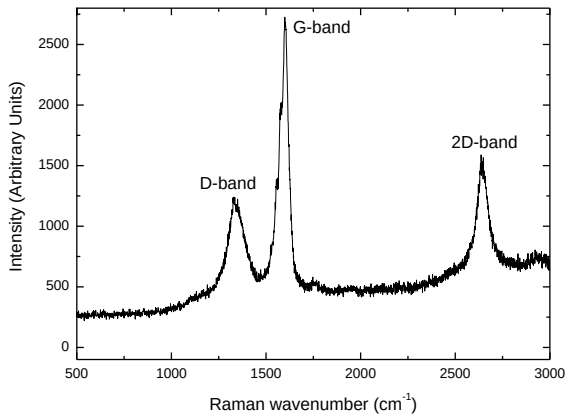

Figure 5 Typical Raman spectra for (a) a high modulus carbon fibre, (b) a low modulus carbon fibre and (c) a low modulus carbon fibre coated with single wall nanotubes (SWNTs)

(a)

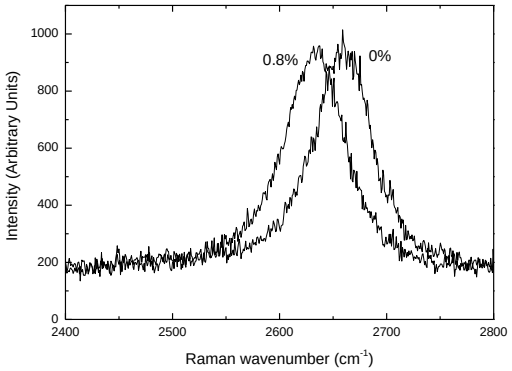

(b)

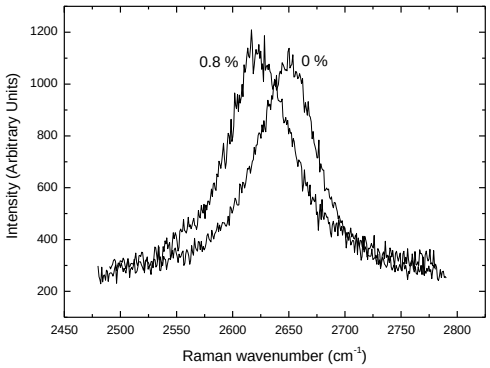

(c)

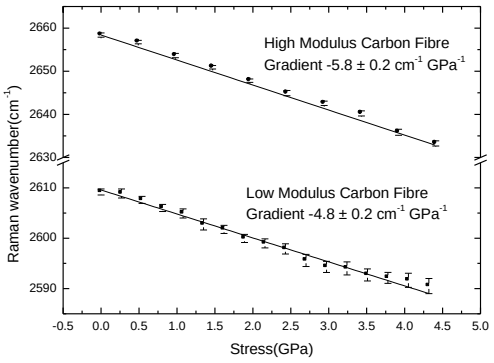

Figure 6 Typical shifts in the position of a band located at ~2660 cm^{-1} (2D) as a function of fibre strain for (a) a high modulus carbon fibre, (b) a low modulus carbon fibre coated with SWNTs and (c) detailed shifts in the peak positions. Solid lines in (c) are linear regressions to the data.

(a)

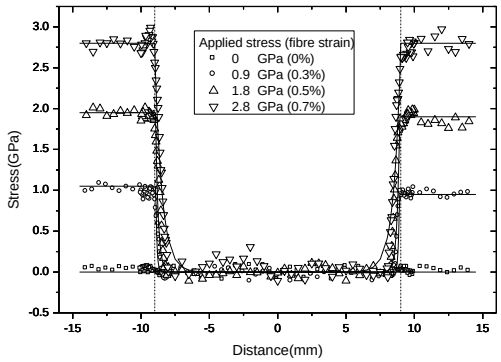

(b)

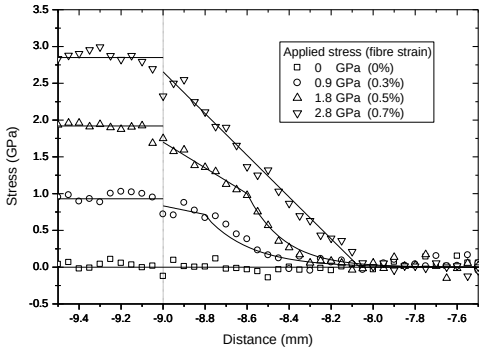

(c)

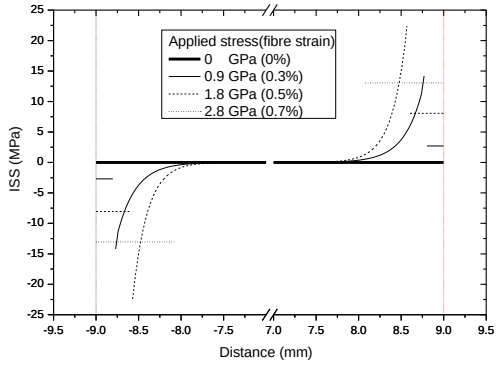

Figure 7 Typical stress distributions through a thin film epoxy resin-high modulus carbon fibre model composite (a) across the whole fibre-matrix interface, (b) re-scaled near to the fibre entry point into the matrix and (c) the interfacial shear stress (ISS) across the whole fibre-matrix interface. Solid lines in (a) are Eqn. 1 and in (b) are Eqns. 1 and 4.

(a)

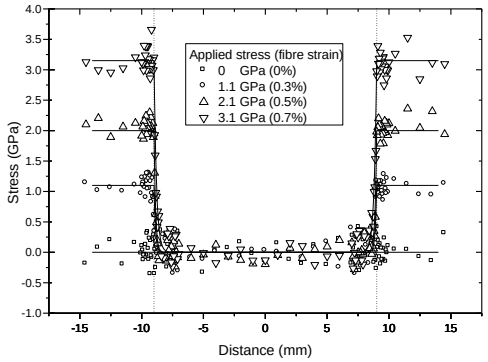

(b)

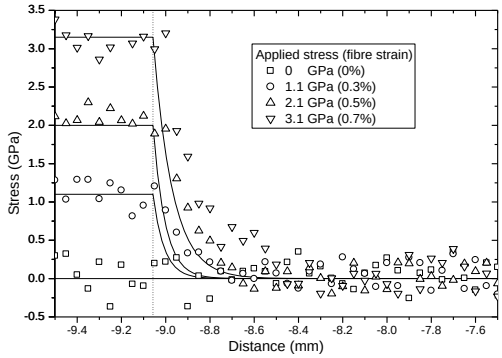

(c)

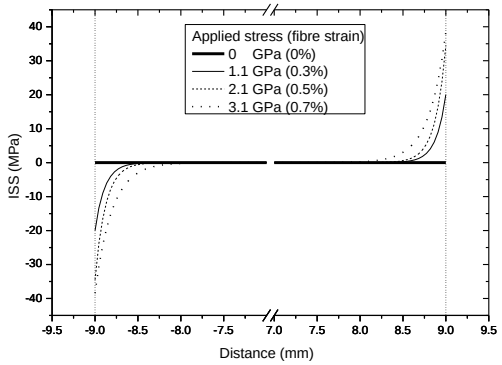

Figure 8 Typical stress distributions through a thin film epoxy resin-high modulus carbon fibre (coated with SWNTs) model composite (a) across the whole fibre-matrix interface, (b) close up near to the fibre entry point into the matrix and (c) the interfacial shear stress (ISS) across the whole fibre-matrix interface. Solid lines in (a) and (b) are Eqn. 1.

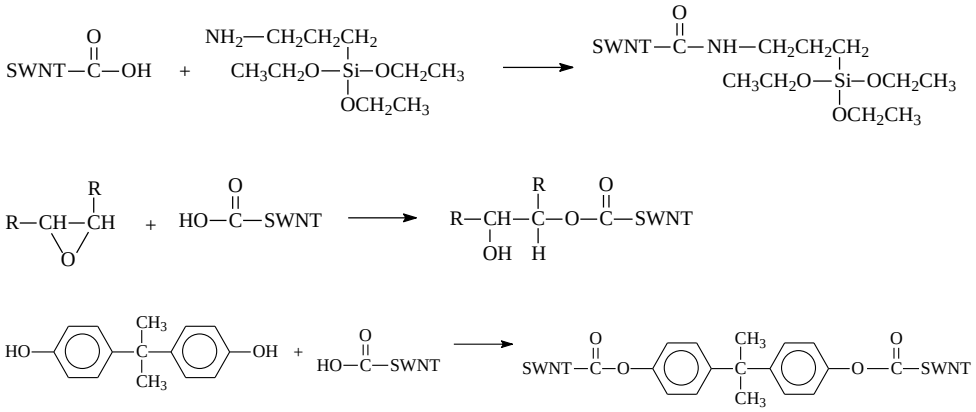

Figure 9 Proposed reactions occurring with carboxylated single walled nanotubes (SWNTS) and components of the epoxy resin.

(a)

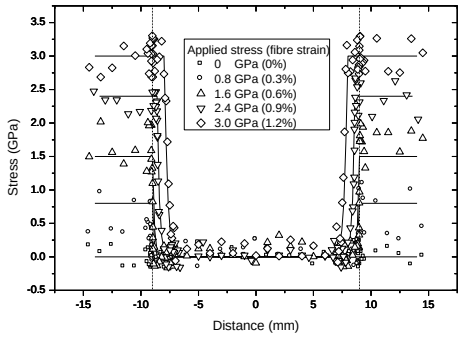

(b)

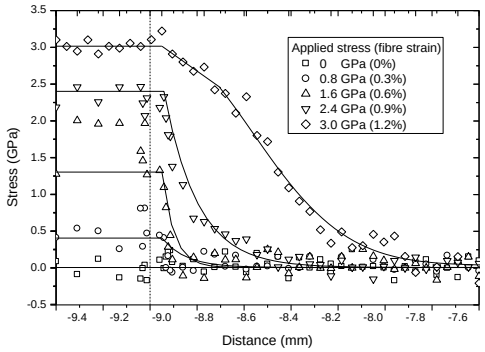

(c)

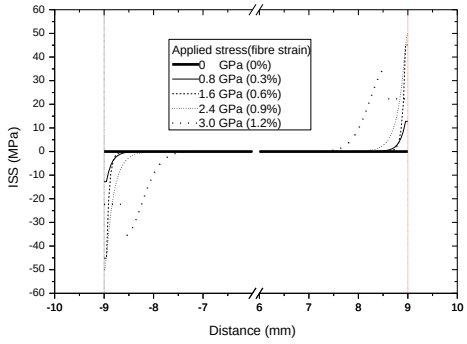

Figure 10 Typical stress distributions through a thin film epoxy resin-low modulus carbon fibre (coated with SWNTs) model composite (a) across the whole fibre-matrix interface, (b) r near to the fibre entry point into the matrix and (c) the interfacial shear stress (ISS) across the whole fibre-matrix interface. Solid lines in (a) are Eqn. 1 and in (b) are Eqns. 1 and 4.

Table 1 Mean mechanical properties for high modulus and low modulus carbon fibres.

	Mean mechanical properties		
Fibre type	Young's Modulus (GPa)	Breaking Stress (GPa)	Breaking Strain (%)
High Modulus Carbon Fibre	451.1 ± 0.7	3.75 ± 0.31	0.95 ± 0.07
Low Modulus Carbon Fibre	264.8 ± 0.4	5.47 ± 0.27	1.74 ± 0.09

Table 2 Maximum interfacial shear stress (ISS) values for model composites with different fibre treatments using single wall nanotubes (SWNTs)

Fibre Type	Treatment	Maximum ISS (MPa)
High modulus carbon fibre	Without SWNTs	22.5 ± 0.2
	With SWNTs	38.4± 0.1
Low modulus carbon fibre	With SWNTs	51.1± 0.2